JOINT EUROPEAN TORUS JET

JET–P(91)15

B. Wolle, L-G Eriksson, K. Htibner, P.D. Morgan, H.W. Morsi,
G. Sadler, M. G von Hellermann and JET Team

Neutron Rate Interpretation for Neutral Beam Heated Tokamaks

"This document contains JET information in a form not yet suitable for publication. The report has been prepared primarily for discussion and information within the JET Project and the Associations. It must not be quoted in publications or in Abstract Journals. External distribution requires approval from the Publications Officer, JET Joint Undertaking, Abingdon, Oxon, OX14 3EA, UK".

"Enquiries about Copyright and reproduction should be addressed to the Publications Officer, EFDA, Culham Science Centre, Abingdon, Oxon, OX14 3DB, UK."

The contents of this preprint and all other JET EFDA Preprints and Conference Papers are available to view online free at www.iop.org/Jet. This site has full search facilities and e-mail alert options. The diagrams contained within the PDFs on this site are hyperlinked from the year 1996 onwards.

Neutron Rate Interpretation for Neutral Beam Heated Tokamaks

B. Wolle[1], L-G Eriksson, K. Htibner[1], P.D. Morgan, H.W. Morsi,
G. Sadler, M. G von Hellermann and JET Team*

JET-Joint Undertaking, Culham Science Centre, OX14 3DB, Abingdon, UK

[1]Institute for Applied Physics, Heidelberg University, D-6900 Heidelberg, Germany
** See Appendix 1*

Preprint of Paper to be submitted for publication in
Plasma Physics and Controlled Fusion (Letter to the Editor)

NEUTRON RATE INTERPRETATION FOR NEUTRAL BEAM HEATED TOKAMAKS

B. Wolle*, L.-G. Eriksson, K. Hübner*, P.D. Morgan, H.W. Morsi, G. Sadler and M.G. von Hellermann

JET Joint Undertaking, Abingdon, Oxon., OX14 3EA, UK
*Institute for Applied Physics, Heidelberg University, D-6900 Heidelberg, Germany

ABSTRACT

It is of great interest to determine the deuteron temperature or density in tokamak fusion plasmas from total neutron rate measurements. This can be done easily during ohmic heating or H° injection, where the velocity distribution function of the plasma deuterons is Maxwellian. However, during D° injection the distribution function is highly non-Maxwellian and until now deuteron temperatures or denstities could only be evaluated with the aid of complex codes. Here we present a fast interpretation code using a Fokker-Planck formalism and identify the parameter ranges where deuteron temperatures or densities can be determined from neutron rate measurements during neutral beam heating. As an example of its application, ion temperatures and densities are evaluated for JET discharges.

1. INTRODUCTION

Neutron diagnostics offer the most direct way to obtain information about the deuterons in fusion plasmas. Thus neutron diagnostics are of increasing importance for future fusion plasmas and efforts are being made to improve the present methods for interpreting neutron signals. The most natural procedure would be to determine deuteron densities from neutron rate measurements and deuteron temperatures from neutron energy spectra. But as neutron spectra are not always (and never in a simple way) available while, on the other hand, the deuteron density can be derived from electron density, Z_{eff}-measurements and impurity composition, there is much interest in determining deuteron temperatures from neutron rate measurements. This is a quite straightforward and simple procedure for thermal plasmas. For auxiliary heated plasmas, information on the deuteron temperature has as yet been accessible

only by using complex and time-consuming codes, such as TRANSP (HAWRYLUK, 1980; GOLDSTON et al., 1981), which attempt to obtain consistency between all measured plasma parameters within small variations of their values. Such plasmas have a highly non-Maxwellian deuteron velocity distribution and therefore an enhanced fusion reactivity which does not depend in a simple manner on the deuteron temperature. Even the use of the term "temperature" is quite questionable in this case. To be precise, we define the deuteron temperature by an asymptotic (and isotropic) Maxwellian part at low velocities in the actual deuteron velocity distribution. The distribution function is thus artificially divided into two parts, one of which is the thermal background plasma and the other is considered as the "beam" part in the distribution. In this sense, the local neutron rate and the local reactivities can be split into thermal, beam-thermal and beam-beam components. But one has always to keep in mind that this is an entirely artificial splitting of the unique ensemble of deuterons in the plasma.

2. REACTIVITIES

The local neutron rate Y for a plasma containing ion species of type (i) and (j), e.g. deuterons and deuterons or tritons, is given by:

$$Y = \frac{n_i n_j}{1+\delta_{ij}} \langle \sigma v \rangle_{ij} \tag{1}$$

where n_i and n_j are the densities of the interacting particles and δ_{ij} is the Kronecker symbol. The reactivity $\langle \sigma v \rangle_{ij}$ is in general given by the 6-dimensional integral:

$$\langle \sigma v \rangle_{ij} = \iint f_i(\vec{v}) f_j(\vec{v}') \sigma(|\vec{v} - \vec{v}'|) |\vec{v} - \vec{v}'| d^3\vec{v} d^3\vec{v}' \tag{2}$$

where $f_i(\vec{v})$ and $f_j(\vec{v}')$ are the normalised distribution functions, σ is the cross-section and $|\vec{v} - \vec{v}'|$ is the velocity of impact. In the case of neutral beam injection, the distribution function $f(\vec{v})$ can be written as the sum of a thermal part $f_t(\vec{v})$ and a non-thermal part $f_b(\vec{v})$ due to the beam as mentioned above:

$$f(\vec{v}) = f_t(\vec{v}) + f_b(\vec{v}). \tag{3}$$

The corresponding densities are n_D, n_t and n_b. The reactivity $\langle \sigma v \rangle$ may then be written as the sum of the different reactivities:

$$\langle \sigma v \rangle = \langle \sigma v \rangle_{tt} + \langle \sigma v \rangle_{bt} + \langle \sigma v \rangle_{bb}. \tag{4}$$

The first term determines the thermal reactivity of the background plasma, the second one describes the reactivity between the fast particles and the background plasma and the last one the reactivity of the fast particles themselves. This leads to the three corresponding neutron rates Y_{tt} (thermal), Y_{bt} (beam-thermal) and Y_{bb} (beam-beam). The determination of those reactivities in general requires the evaluation of a 6-dimensional integral. CORDEY et al. (1978), however, showed that considerable analytic simplification for toroidally confined plasmas can be achieved by symmetry assumptions and expansion of the distribution functions $f(v,\mu)$, where $v = |\vec{v}|$ and $\mu = v_{\parallel} / v = \cos\theta$ is the cosine of the pitch angle, in Legendre polynomials P_n as:

$$f(v,\mu) = \sum_{n=0}^{\infty} a_n(v) P_n(\mu)$$

thus reducing the number of integrations to be performed. For the above reactivities one obtains the following expressions:

$$\langle \sigma v \rangle_{tt} = \frac{2}{\sqrt{\pi}} \left(\frac{m}{2kT} \right)^{3/2} \int_o^{\infty} w^3 \sigma(w) e^{-\frac{mw^2}{2kT}} dw, \tag{5a}$$

$$\langle \sigma v \rangle_{bt} = 8\sqrt{\pi} \int_o^{\infty} a_o(v) \sqrt{\frac{mv^2}{2kT}} e^{-\frac{mv^2}{2kT}} \int_o^{\infty} w^2 \sigma(w) \sinh\left(\frac{mvw}{kT} \right) e^{-\frac{mw^2}{2kT}} dw dv, \tag{5b}$$

$$\langle \sigma v \rangle_{bb} = 8\pi^2 \sum_{n=1}^{\infty} \frac{1}{2n+1} \int_o^{\infty} v^2 a_n(v) \int_o^{\infty} v'^2 b_n(v') \int_{-1}^{1} P_n(\mu_{12}) \sigma(u) u d\mu_{12} dv' dv \tag{5c}$$

with $\mu_{12} = \cos(\theta' - \theta)$, $w = |v - v'|$, $m = m_i m_j / (m_i + m_j)$ and $u^2 = v^2 + v'^2 - 2vv'\mu_{12}$. It should be mentioned that the zeroth order eigenfunctions $a_o(v)$, $b_o(v')$ of this expansion are the pitch-angle-averaged distribution functions:

$$a_o(v) \equiv F(v) = \frac{1}{2} \int_{-1}^{1} f(v,\mu) d\mu. \tag{6}$$

3. STRUCTURE OF THE INTERPRETATION CODE

We have developed a code called NR-FPS (Neutron Rate-Fokker-Planck-Solver) which has a fully modular structure. A software module which is easy to adapt to changes in central data banks or to newly available diagnostics data reads all the input data which, apart from the neutral beam deposition, are measured. The local distribution functions and the reactivities are determined in the main module. In the interpretation module, one of the three local parameters comprising neutron rate Y, ion temperature T_i, and deuteron density n_D, can always be calculated, the other two being taken as alternate inputs to iterate the value of the plasma parameter of interest. The code thus allows not only the determination of T_i or n_D, but also prediction of neutron rates and neutron emission profiles and therefore detailed studies of the influence of relevant plasma parameters on the neutron rate.

4. FOKKER-PLANCK MODEL

To calculate the non-thermal distribution function, we have chosen the simplified steady-state model as given by ANDERSON et al. (1988), in order to speed up calculations for online applications. We extended this one dimensional model to two dimensions v and μ in order to calculate beam-beam reactivities. The Fokker-Planck equation is:

$$\frac{\partial f(v,\mu)}{\partial t} = C(f(v,\mu)) + S(v,\mu) - L(v) = 0 \qquad (7)$$

where C is the collision operator (see for instance STIX, 1975), S is the source of injected particles with given energy and injection angle and L is a particle loss term.

Usually, the diffusion coefficients in the collision operator are calculated using the Maxwellian velocity distribution of the background plasma in the Rosenbluth potentials. For the electrons we can assume throughout a Maxwellian distribution with the measured electron temperature. To estimate the effect of the non-Maxwellian deuteron distribution on the particle relaxation we can use optionally a self-consistent solution which takes into account the actual distribution function in the collision operator. Thus the Fokker-Planck equation becomes a non-linear integro-differential equation which is solved using an iteration technique, taking the initial distribution as Maxwellian.

Figure 1 shows the beam part of the pitch-angle averaged deuteron distribution function F_b (Eq.6) as a function of energy calculated with a Maxwellian deuteron distribution (dotted line) and with the iteration procedure (solid line) for $T_e = T_i = 2keV$, $n_e = 4 \times 10^{13}cm^{-3}$, $n_D/n_e = 0.65$, injection source rate $s_0 = 5.96 \cdot 10^{13}sec^{-1}$ and $E_{inj} = 40$ keV.

The effect of the self-consistent treatment on the distribution function and the reactivity is rather small. The plasma parameters were chosen to give a relatively large final difference in the calculated neutron rate, which in this case is 6%, while the typical difference for JET is smaller than 2%.

At first the electrons, which are always Maxwellian, dominate the particle relaxation for high velocities. Around and below the transition energy (cgs):

$$\frac{1}{2}mv_\alpha^2 = 14.8\, kT_e \left[\frac{A^{3/2}}{n_e} \sum_j \frac{n_i z_j}{A_j} \right]^{2/3} \tag{8}$$

where A and A_j are the atomic masses of the test and j species of field ions, n_e is in cm^{-3} and T_e in eV, the ion collisions become more important and the use of the true deuteron distribution function results in an overall reduction of the relative velocities and in a lower background density. This leads to a retardation of the relaxation process and thus to an enhancement of the deuteron population in the distribution function around $\frac{1}{2}\, mv_\alpha^2$.

5. RANGES OF APPLICATION

The neutron rate depends in a complicated manner on the different plasma parameters, and small changes in the input data can have a strong influence. The relative change in the neutron rate Y due to variations of the four most important input parameters T_e, T_i, n_D and injection source rate s_0 is given by:

$$\frac{dY}{Y} = \frac{T_e \partial Y}{Y \partial T_e} \frac{dT_e}{T_e} + \frac{T_i \partial Y}{Y \partial T_i} \frac{dT_i}{T_i} + \frac{n_D \partial Y}{Y \partial n_D} \frac{dn_D}{n_D} + \frac{s_o \partial Y}{Y \partial s_o} \frac{ds_o}{s_o}. \tag{9}$$

The sensitivity factors K_e, K_i, K_D and K_S which describe the influence of electron and ion temperature, deuteron density and source rate:

$$K_e = \frac{\partial Y}{Y \partial T_e}, \quad K_i = \frac{\partial Y}{Y \partial T_i}, \quad K_D = \frac{\partial Y}{Y \partial n_D}, \quad K_s = \frac{\partial Y}{Y \partial s_o}. \tag{10}$$

are again functions of all the other plasma parameters. It should be pointed out that the higher the value of one of these factors, the stronger is the neutron rate dependence on the corresponding plasma parameter. By calculating 1,200 points in the 4-dimensional parameter space $Y(T_e, T_i, n_D, s_o)$ (5 for T_i, 5 for T_e, 4 for s_o, 3 for n_e and 4 for n_D), we obtained empirical fit-functions for the sensitivity factors. These fit-functions can be used to determine the range of applications for neutron interpretation calculations. Figure 2 shows the sensitivity functions of T_e, T_i, n_D and s_o for 80keV injection energy with a power density typical for JET of 0.77 W/cm^3 plotted in a n_D vs. T_i diagram, together with measured data points from the JET data base. The curves for the sensitivity of the neutron rate on the ion temperature are plotted for $K_i = 0.15$ and 0.20, meaning that a change of 15% or 20% in neutron rate is caused by a change in T_i by 1keV. The curves for $K_e = 0.2$ and $K_D = 0.2$, where the latter signifies a 20% change due to a change by 10^{19}m^{-3} in n_D, are also plotted. In addition, the curve for $K_i = K_e$ is shown. For points belonging to this curve the neutron rate is influenced equally by T_i and T_e, while the dependence on T_e dominates for points below and the dependence on T_i dominates for points above this line.

Most of the measured data points are located below $K_i = K_e$ and thus for these points the influence of T_e dominates over the dependence on the ion temperature. The weak dependence of the neutron rate on T_i is due to the fact that the non-Maxwellian part of the distribution function results from the relaxation process of the injected particles and thus F_b mostly depends on T_e, s_o, n_e and E_{inj}. If the neutron flux consists mainly of beam-beam and beam-thermal neutrons, which for example is the case for low deuteron density plasmas, then T_e influences the neutron rate more than T_i.

The shaded areas in Fig. 2 show where one of the plasma parameters T_e, T_i and n_D has a stronger influence on the neutron rate than the others and thus mark optimum parameter regions for interpretation calculations. The picture indicates that the ion temperature can hardly be determined for high temperature plasmas with low densities such as hot ion modes. However, the deuteron density can be calculated with good accuracy by numerical analysis in

this case. On the other hand, the ion temperature can be obtained from interpretation calculations for medium temperature, medium and high deuteron density plasmas if the other plasma parameters are measured with sufficient accuracy. A comparison with the experimental data shows that the ion temperature can be calculated with reasonable accuracy only in a very limited range, while interpretation calculations for n_D can be performed for most discharges.

The errors in the temperatures and densities derived from neutron rates depend on the sensitivity factors (Eq.9) and the errors in the input data and are determined by a variation of the input values within their error range. As an order of magnitude, for the deuteron temperature in the shaded T_i-region of Fig. 2 we expect an error approximately twice as large as the error in the input data. But this error increases strongly with decreasing density. On the other hand, the error in deuteron density derived from the neutron rate is in the same order as the errors in the input data, and decreases with increasing temperature and decreasing deuteron density.

6. EXAMPLES OF APPLICATION

Neutron rate interpretation calculations have been carried out for various JET discharges with 80keV deuterium injection. As a representative example of an evaluation of ion temperature, we present the result for the H-mode discharge #17160 with P_{inj} = 6.7MW. With temperatures of about 3-4keV and central deuteron densities of $2.5\text{-}3.5\times10^{19}m^{-3}$, this pulse belongs according to Fig. 2, to a parameter range where the critical parameters are T_e and n_D. The sensitivity factor for T_i is K_i = 0.1 approximately and thus an ion temperature determination is possible for time points with low dilution. Taking the measured T_e- and n_e-profiles, the calculated deposition profiles from PENCIL (STUBBERFIELD et al., 1987) and the plasma composition deduced from Z_{eff} assuming a hydrogen density of n_H = 5% of the ion density and a carbon to oxygen ratio of n_C/n_O = 5.0, we calculate a central ion temperature of $T_i(0) = (3.14 \pm 0.20)$keV. The measured values are (3.6 ± 0.5)keV from charge exchange recombination spectroscopy (CXRS) (BOILEAU et al., 1989) and (3.0 ± 0.3)keV from X-ray crystal spectrometry (XCS) (MORSI et al., 1990). Alternatively, taking the measured T_i-profiles, the central deuteron density and thus the ratio n_D/n_e can be determined. Figure 3a

shows measured n_D/n_e ratios from CXRS assuming n_H/n_{ions} of 5% and 10% in the plasma and from the visible bremsstrahlung Z_{eff} (HAL) (MORGAN, 1988) together with our results (calc.).

For the hot ion H-mode discharge #18757, which has been discussed in much detail before (ADAMS et al, 1990; BALET et al., 1990; WATKINS et al., 1989), a temperature determination from neutron rates is not possible since the neutron rate depends weakly on T_i for high temperatures and low densities. In this parameter region, instead, the neutron rate strongly depends on n_D. In Fig. 3b again measured ratios n_D/n_e from CXRS and HAL are plotted as a function of time together with the results of our calculation (calc.) showing again good agreement between all independent diagnostic methods.

CONCLUSIONS

With our fast interpretation software the determination of ion temperature or deuteron density from neutron rate measurements is extended to neutral-beam- heated tokamak discharges. Based on a sensitivity study, the error bars on an interpretation calculation can be related to the errors in the measured input plasma data. This fixes the range of application for a T_i - or n_D determination for a given accuracy in measurements. In general, a T_i determination is possible for plasmas with moderate temperatures and medium to high deuterium densities. The determination of n_D offers a much wider range of application covering most of the experimentally accessible plasma regimes.

The errors of the evaluated plasma parameters can be smaller than those from other diagnostics, provided the numerous input plasma parameters are measured with sufficient accuracy. This demonstraties the potential of our methods for future fusion plasma diagnostics and experimental cross-checks.

Acknowledgements

One of the authors, B. Wolle, would like to thank JET Theory Division for its hospitality and in particular, Prof. D. Düchs and Dr. T. Stringer for their encouraging interest in this work.

References

Adams, J.M., Balet, B., Boyd, D., Campbell, D.J., Challis, C., Christiansen, J.P., Cordey, J.G., Core, W.G.F., Costley, A, Cottrell, G., Edwards, A., Elevant, T., Eriksson, L., Hellsten, T., Jarvis, O.N., Lallia, P., Lawson, K., Lowry, L., Morgan, P., Nielsen, P., Sadler, G., Start, D., Thomas, P., Thomsen, K., von Hellermann, M. and Weisen, H., JET-P(90)10, to be published in Nucl. Fusion.

Anderson, D., Core, W., Eriksson, L.-G., Hamnén, H., Hellsten, T. and Lisak, M., Physica Scripta, 37, 83 (1988).

Balet, B., Boyd, D., Campbell, D.J., Challis, C., Christiansen, J.P., Cordey, J.G., Core, W.G.F., Costley, A, Cottrell, G., Edwards, A., Elevant, T., Eriksson, L., Hellsten, T., Jarvis, O.N., Lallia, P., Lawson, K., Lowry, L., Morgan, P., Nielsen, P., Sadler, G., Start, D., Thomas, P., Thomsen, K., von Hellermann, M. and Weisen, H., Nucl. Fusion, 30, 2029 (1990).

Boileau, A., von Hellermann, M., Horton, L. and Summers, H.P., Plasma Phys. Controlled Fusion 31,779 (1989).

Cordey, J.G., Marx, K.D., McCoy, M.G., Mirin, A.A. and Resnik, M.E., J. Comput. Phys., 28, 115 (1978).

Goldston, R.J., McCune, D.C., Towner, H.H., Davis, S.L., Hawryluk, R.J., Schmidt, G.L., J. Comput. Phys. 43, 61 (1981).

Hawryluk, R.J. (Varenna 1980) EUR FU BRU/XII 476/80.

Morgan, P.D., Proc. 15th Eur. Conf. 1988, Vol. 12B, Part I, 139 (1988).

Morsi, H.W., von Hellermann, M.G., Zastrow, K.-D., et al., Proc. 117th Eur. Conf. Contr. Fusion and Plasma Heating 1990, Vol.14B, 1608 (1990).

Stix, T.H., Nucl. Fusion, 15, 737 (1975).

Stubberfield, P.M. and Watkins, M.L., JET Experimental Department Research Note DPA(06)87, Multiple Pencil Beam (1987).

Watkins, M.L., Balet, B., Bathnagar, V.P., Cordey, J.G., Hammett, G.W., Hellsten, T., Keilhacker, M., Milora, S.L., Morgan, P.D., Sack, C., Schmidt, G.L., Taroni, A., Thomas, P.R., Thomsen, K., Tibone, F., von Hellermann, M. and Weisen, H., Plasma Phys. Controlled Fusion, 31, 1713 (1989).

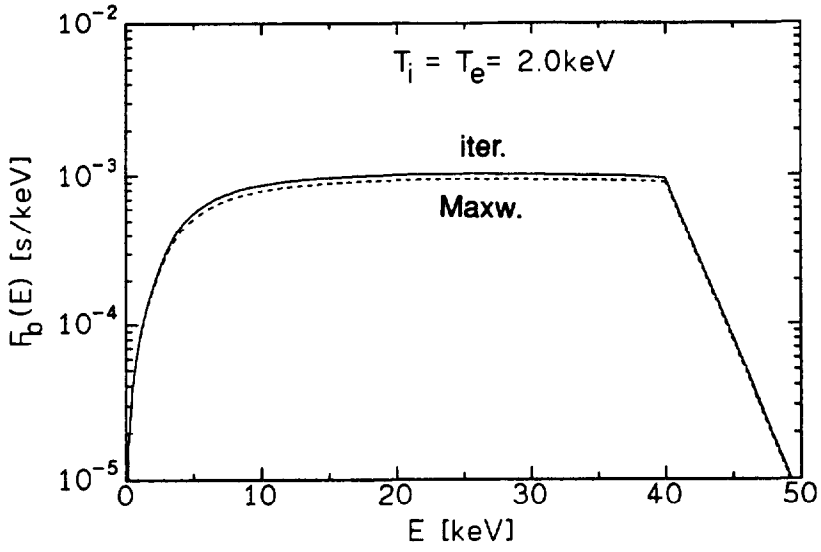

Fig. 1 Distribution functions calculated using classical Rosenbluth potentials (dashed) and by iteration (solid).

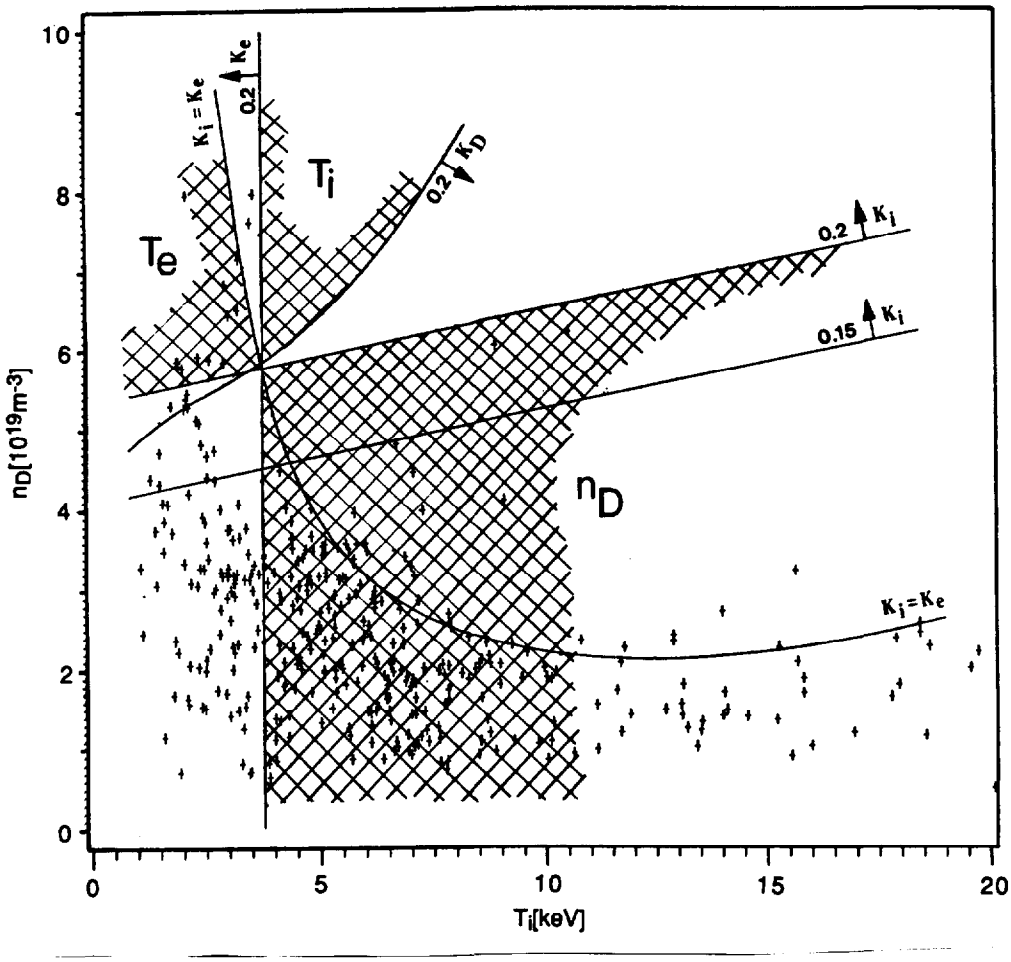

Fig. 2: Sensitivity functions for 80keV injection energy with 0.77 W/cm^3 power density. Plotted are functions for $K_i = 0.15, 0.2$, $K_D = 0.2$ and $K_i = K_e$. The arrows point to the direction of increasing K and the shaded areas mark regions where one parameter out of K_i, K_e, K_D is largest. The crosses denote JET discharges from 1988 and 1989.

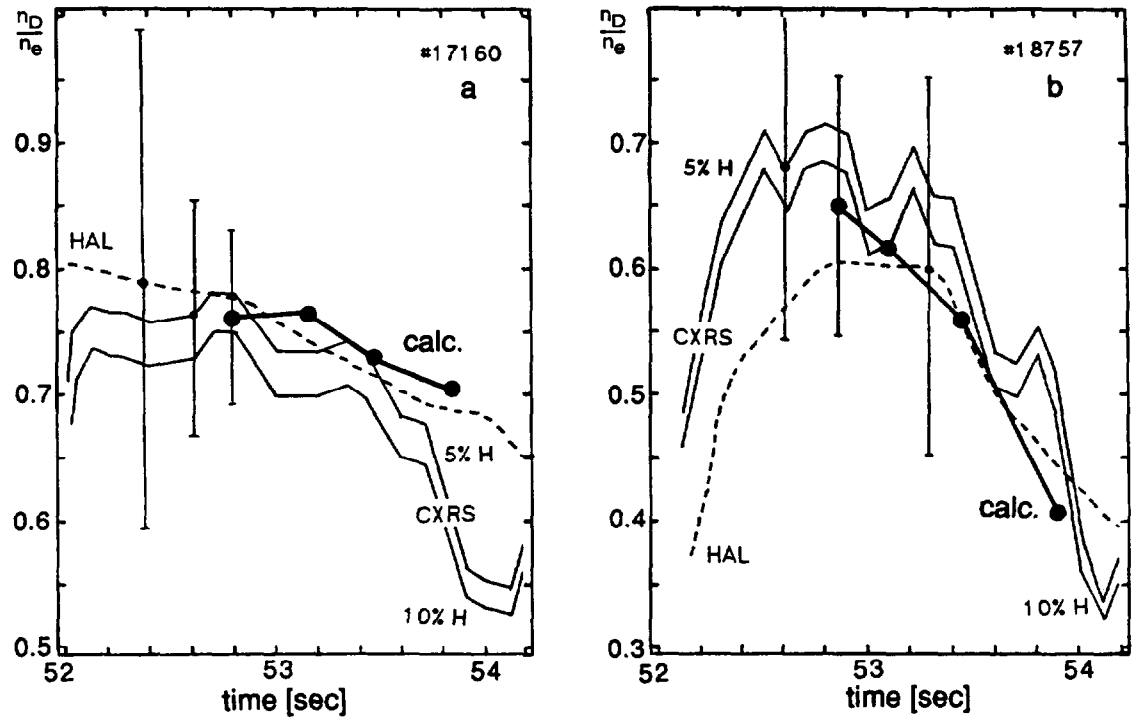

Fig. 3: Dilution n_D/n_e as a function of time from CXRS diagnostics under the assumption of 5% and 10% H^+ concentration, from visible bremsstrahlung (HAL) and the calculated n_D/n_e ratios (connected points) for the discharges #17160 (a) and 18757 (b).

APPENDIX 1.

THE JET TEAM

JET Joint Undertaking, Abingdon, Oxon, OX14 3EA, U.K.

J.M.Adams[1], F.Alladio[4], H.Altmann, R.J.Anderson, G.Appruzzese, W.Bailey, B.Balet, D.V.Bartlett, L.R.Baylor[24], K.Behringer, A.C.Bell, P.Bertoldi, E.Bertolini, V.Bhatnagar, R.J.Bickerton, A.Boileau[3], T.Bonicelli, S.J.Booth, G.Bosia, M.Botman, D.Boyd[31], H.Brelen, H.Brinkschulte, M.Brusati, T.Budd, M.Bures, T.Businaro[4], H.Buttgereit, D.Cacaut, C.Caldwell-Nichols, D.J.Campbell, P.Card, J.Carwardine, G.Celentano, P.Chabert[27], C.D.Challis, A.Cheetham, J.Christiansen, C.Christodoulopoulos, P.Chuilon, R.Claesen, S.Clement[30], J.P.Coad, P.Colestock[6], S.Conroy[13], M.Cooke, S.Cooper, J.G.Cordey, W.Core, S.Corti, A.E.Costley, G.Cottrell, M.Cox[7], P.Cripwell[13], F.Crisanti[4], D.Cross, H.de Blank[16], J.de Haas[16], L.de Kock, E.Deksnis, G.B.Denne, G.Deschamps, G.Devillars, K.J.Dietz, J.Dobbing, S.E.Dorling, P.G.Doyle, D.F.Düchs, H.Duquenoy, A.Edwards, J.Ehrenberg[14], T.Elevant[12], W.Engelhardt, S.K.Erents[7], L.G.Eriksonn[5], M.Evrard[2], H.Falter, D.Flory, M.Forrest[7], C.Froger, K.Fullard, M.Gadeberg[11], A.Galetsas, R.Galvao[8], A.Gibson, R.D.Gill, A.Gondhalekar, C.Gordon, G.Gorini, C.Gormezano, N.A.Gottardi, C.Gowers, B.J.Green, F.S.Griph, M.Gryzinski[26], R.Haange, G.Hammett[6], W.Han[9], C.J.Hancock, P.J.Harbour, N.C.Hawkes[7], P.Haynes[7], T.Hellsten, J.L.Hemmerich, R.Hemsworth, R.F.Herzog, K.Hirsch[14], J.Hoekzema, W.A.Houlberg[24], J.How, M.Huart, A.Hubbard, T.P.Hughes[32], M.Hugon, M.Huguet, J.Jacquinot, O.N.Jarvis, T.C.Jernigan[24], E.Joffrin, E.M.Jones, L.P.D.F.Jones, T.T.C.Jones, J.Källne, A.Kaye, B.E.Keen, M.Keilhacker, G.J.Kelly, A.Khare[15], S.Knowlton, A.Konstantellos, M.Kovanen[21], P.Kupschus, P.Lallia, J.R.Last, L.Lauro-Taroni, M.Laux[33], K.Lawson[7], E.Lazzaro, M.Lennholm, X.Litaudon, P.Lomas, M.Lorentz-Gottardi[2], C.Lowry, G.Magyar, D.Maisonnier, M.Malacarne, V.Marchese, P.Massmann, L.McCarthy[28], G.McCracken[7], P.Mendonca, P.Meriguet, P.Micozzi[4], S.F.Mills, P.Millward, S.L.Milora[24], A.Moissonnier, P.L.Mondino, D.Moreau[17], P.Morgan, H.Morsi[14], G.Murphy, M.F.Nave, M.Newman, L.Nickesson, P.Nielsen, P.Noll, W.Obert, D.O'Brien, J.O'Rourke, M.G.Pacco-Düchs, M.Pain, S.Papastergiou, D.Pasini[20], M.Paume[27], N.Peacock[7], D.Pearson[13], F.Pegoraro, M.Pick, S.Pitcher[7], J.Plancoulaine, J-P.Poffé, F.Porcelli, R.Prentice, T.Raimondi, J.Ramette[17], J.M.Rax[27], C.Raymond, P-H.Rebut, J.Removille, F.Rimini, D.Robinson[7], A.Rolfe, R.T.Ross, L.Rossi, G.Rupprecht[14], R.Rushton, P.Rutter, H.C.Sack, G.Sadler, N.Salmon[13], H.Salzmann[14], A.Santagiustina, D.Schissel[25], P.H.Schild, M.Schmid, G.Schmidt[6], R.L.Shaw, A.Sibley, R.Simonini, J.Sips[16], P.Smeulders, J.Snipes, S.Sommers, L.Sonnerup, K.Sonnenberg, M.Stamp, P.Stangeby[19], D.Start, C.A.Steed, D.Stork, P.E.Stott, T.E.Stringer, D.Stubberfield, T.Sugie[18], D.Summers, H.Summers[20], J.Taboda-Duarte[22], J.Tagle[30], H.Tamnen, A.Tanga, A.Taroni, C.Tebaldi[23], A.Tesini, P.R.Thomas, E.Thompson, K.Thomsen[11], P.Trevalion, M.Tschudin, B.Tubbing, K.Uchino[29], E.Usselmann, H.van der Beken, M.von Hellermann, T.Wade, C.Walker, B.A.Wallander, M.Walravens, K.Walter, D.Ward, M.L.Watkins, J.Wesson, D.H.Wheeler, J.Wilks, U.Willen[12], D.Wilson, T.Winkel, C.Woodward, M.Wykes, I.D.Young, L.Zannelli, M.Zarnstorff[6], D.Zasche[14], J.W.Zwart.

PERMANENT ADDRESS

1. UKAEA, Harwell, Oxon. UK.
2. EUR-EB Association, LPP-ERM/KMS, B-1040 Brussels, Belgium.
3. Institute National des Récherches Scientifique, Quebec, Canada.
4. ENEA-CENTRO Di Frascati, I-00044 Frascati, Roma, Italy.
5. Chalmers University of Technology, Göteborg, Sweden.
6. Princeton Plasma Physics Laboratory, New Jersey, USA.
7. UKAEA Culham Laboratory, Abingdon, Oxon. UK.
8. Plasma Physics Laboratory, Space Research Institute, Sao José dos Campos, Brazil.
9. Institute of Mathematics, University of Oxford, UK.
10. CRPP/EPFL, 21 Avenue des Bains, CH-1007 Lausanne, Switzerland.
11. Risø National Laboratory, DK-4000 Roskilde, Denmark.
12. Swedish Energy Research Commission, S-10072 Stockholm, Sweden.
13. Imperial College of Science and Technology, University of London, UK.
14. Max Planck Institut für Plasmaphysik, D-8046 Garching bei München, FRG.
15. Institute for Plasma Research, Gandhinagar Bhat Gujat, India.
16. FOM Instituut voor Plasmafysica, 3430 Be Nieuwegein, The Netherlands.
17. Commissiariat à L'Energie Atomique, F-92260 Fontenay-aux-Roses, France.
18. JAERI, Tokai Research Establishment, Tokai-Mura, Naka-Gun, Japan.
19. Institute for Aerospace Studies, University of Toronto, Downsview, Ontario, Canada.
20. University of Strathclyde, Glasgow, G4 ONG, U.K.
21. Nuclear Engineering Laboratory, Lapeenranta University, Finland.
22. JNICT, Lisboa, Portugal.
23. Department of Mathematics, Univeristy of Bologna, Italy.
24. Oak Ridge National Laboratory, Oak Ridge, Tenn., USA.
25. G.A. Technologies, San Diego, California, USA.
26. Institute for Nuclear Studies, Swierk, Poland.
27. Commissiariat à l'Energie Atomique, Cadarache, France.
28. School of Physical Sciences, Flinders University of South Australia, South Australia SO42.
29. Kyushi University, Kasagu Fukuoka, Japan.
30. Centro de Investigaciones Energeticas Medioambientales y Techalogicas, Spain.
31. University of Maryland, College Park, Maryland, USA.
32. University of Essex, Colchester, UK.
33. Akademie de Wissenschaften, Berlin, DDR.

CR 88.49.1A